IEEE Access
Multidisciplinary ⋮ Rapid Review ⋮ Open Access Journal

Received May 29, 2022, accepted June 16, 2022, date of publication June 20, 2022, date of current version June 24, 2022.

Digital Object Identifier 10.1109/ACCESS.2022.3184417

Design of Virtual Reference Feedforward Controller for an Active Suspension System

YONGHWAN JEONG[1], YOUNGIL SOHN[2], SEHYUN CHANG[2], AND SEONGJIN YIM[1], (Member, IEEE)

[1]Department of Mechanical and Automotive Engineering, Seoul National University of Science and Technology, Nowon-gu, Seoul 01811, Republic of Korea
[2]Institute of Advanced Technology Development, Hyundai Motor Company, Seongnam-si, Gyeonggi-do 13529, Republic of Korea

Corresponding author: Seongjin Yim (acebtif@seoultech.ac.kr)

This work was supported by Research Program through Hyundai Motor Group.

ABSTRACT This paper presents a method to design a virtual reference feedforward controller (VRFC) for an active suspension system. Generally, it is not easy to apply a feedforward control to an active suspension system because a reference or disturbance is difficult to measure or estimate. Instead of measuring references or disturbances, a virtual reference on heave motion of a sprung mass representing a bump is defined and used for feedforward control in this paper. Feedforward controller with the virtual reference is combined with feedback controllers such as linear quadratic regulator (LQR) and linear quadratic (LQ) static output feedback (SOF) controller. To fully take advantages of the virtual reference for an active suspension system, it is necessary to find optimal parameters of the virtual reference which maximizes control performance. For the purpose, a simulation-based optimization is formulated and solved by a heuristic optimization method. A simulation with a simulation package shows that the proposed VRFC is quite effective in improving the ride comfort with an active suspension system.

INDEX TERMS Active suspension control, virtual reference feedforward control (VRFC), 2-DOF quarter-car model, LQR, LQ SOF control.

NOMENCLATURE

b_s	damping coefficient of suspension.
f	suspension force.
h	height of virtual reference.
J	LQ objective function.
k_s	spring stiffness of suspension.
k_t	tire stiffness.
m_s	sprung mass of quarter-car model.
m_u	unsprung mass of quarter-car model.
u	control input in quarter-car model.
u_{fb}	feedback control input in quarter-car model.
u_{ff}	feedforward control input in quarter-car model.
z_s, $\dot{z}_s$	vertical displacement and velocity of sprung mass.
$z_{s,ref}$	virtual reference on height of sprung mass.
z_u, $\dot{z}_u$	vertical displacement and velocity of unsprung mass.
z_r	road profile acting on unsprung mass.
η	maximum allowable value of each term in J.
μ	mean of virtual reference.
ρ	weight on each term in J.
σ	standard deviation of virtual reference.

The associate editor coordinating the review of this manuscript and approving it for publication was Qi Zhou.

I. INTRODUCTION

Generally, it is considered that the goal of a suspension design for a vehicle is to achieve both ride comfort and road holding [1], [2]. Typically, ride comfort has been evaluated with a vertical acceleration of a sprung mass. For better ride comfort, the vertical acceleration of a sprung mass should be reduced [3], [4]. According to ISO2631-1, the target frequency ranges of the vertical acceleration of a sprung mass span between 4 and 10Hz [4]. This paper will focus on improving ride comfort with an active suspension system.

An active suspension system has been used to reduce the road-induced vertical acceleration and improve the ride comfort by exerting a control force with some actuators. To date, so many papers have been published to design and implement a controller for active suspension [5]–[7]. Most of these papers have adopted only feedback control. On the contrary, there have been fewer papers on feedforward control for an active suspension system. A typical disturbance used

for feedforward control in an active suspension system is a road profile acting on an unsprung mass [7]. LQ optimal control was adopted to design a feedforward controller with a measured or estimated road profile [8], [9]. However, it is difficult to measure or estimate a road profile in real-time. For the reason, there have been few papers on feedforward control with a road profile. On the other hand, a road profile can be measured *a priori* by a look-ahead sensor. With the previewed road profile, a preview control has been applied to date [7], [8]. In fact, most of the papers on feedforward control for an active suspension system have adopted a preview control [7], [10]–[24]. Among them, LQ optimal preview control has been widely adopted for designing a preview controller [10]–[16], [19], [21], [23]. H_∞ optimal preview control, sliding mode control and model predictive control (MPC) were also adopted for preview controller design [13], [17], [18], [20], [22], [24].

The drawback of the preview control for an active suspension system is that it is difficult to measure a road profile *a priori* with a sensor. There are several methods to measure a road profile with look-ahead sensors. The most popular method is to use computer vision with a camera or a laser scanner. For example, a radar and laser scanner were used as a preview sensor for active suspension control [25], [26]. eActive3 developed by Toyota has laser displacement sensors which are located at the front bumper and are angled downward the front of the vehicle. The laser contact point of this sensor is set to a position 1.4 m forward of the center of the front axle [27]. Active Body Control (ABC) developed by Mercedes-Benz in 2007 has laser scanners used for look-ahead scan on road surface [6], [28]. Moreover, Magic Body Control (MBC) developed by the same company in 2013 has the Road Surface Scan function with a stereo camera. It was known that this system can scan road surface up to 15 m ahead of a vehicle at speeds up to 130 km/h [29]. Recent advances in computer vision technology for autonomous driving makes it possible to detect a bump in front of a vehicle with a stereo camera [30]–[32]. The profile of a bump obtained by the stereo camera can be used for preview control. In spite that there are available look-ahead sensors for preview control, installation of these sensors on a mass-produced vehicle requires additional cost and high-performance processor to handle computational burdens. Hence, it is necessary to develop a new method to design a feedforward controller which does not need additional cost and high-performance processor for signal processing on preview sensors for an active suspension system.

This paper presents a virtual reference feedforward control (VRFC) for an active suspension system. Fig. 1 shows the overall control structure for an active suspension system proposed in this paper. In Fig. 1, LQR and LQ SOF control are used as a feedback controller. As shown in Fig. 1, a 2-DOF quarter-car model is adopted as a vehicle model because a controller designed with it can be directly applied to the full-car model [33], [34]. In this paper, a virtual reference on heave motion of a sprung mass representing a bump is

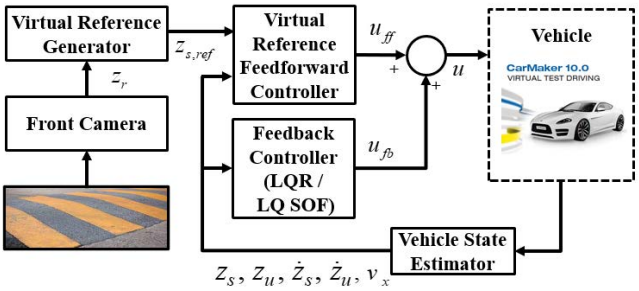

FIGURE 1. Overall control structure with a virtual reference feedforward control for an active suspension system.

defined with an exponential function or a normal distribution, regardless of a real bump profile. A method to generate a desired road height profile was proposed to be used for feedforward compensation in the previous study [20]. As another case, a virtual feedforward controller (VFC) was proposed for periodic disturbances [35], [36]. The VFC proposed in the study was a transfer function with not a reference but a disturbance. Different from the previous studies, the virtual reference proposed in this paper is about not the road profile but the height of a sprung mass. Moreover, the virtual reference has the shape of normal distribution, which has nothing to do with that of a real bump. In other words, the virtual reference does not need information on the shape of a road profile obtained from preview sensors. Hence, it is easier to obtain the virtual reference than a road profile on actual vehicles. The feedforward controller, i.e., VRFC, is designed with the virtual reference. More specifically, the VRFC is just a proportional control (P-control) with the error between the height of a sprung mass and the virtual reference. The VRFC has a single gain for P-control. It is also easy to implement it on actual vehicles. The VRFC is combined with the feedback controllers such as LQR and LQ SOF controller, as shown in Fig. 1.

To maximize the performance of the VRFC, it is necessary to optimize the parameters of the virtual reference and the proportional gain of the VRFC. For this purpose, a simulation-based optimization is formulated to find a virtual reference and control gain which give the optimal performance. A heuristic optimization method is employed for simulation-based optimization. For optimization, several objective functions including the vertical acceleration of a sprung mass, suspension stroke and tire deflection are defined. Several VRFCs designed with 3 objective functions are compared among one another through simulation. When applying the VRFC, the speed variation of a vehicle is important because the optimality of the parameters and gain will be broken if the vehicle speed varies over time. Hence, it is necessary to fix the virtual reference and to optimize the single gain of the P-controller over speed variation. This is also done with a simulation-based optimization. To check the performance of the proposed VRFC for active suspension control, a simulation on CarMaker, a vehicle simulation

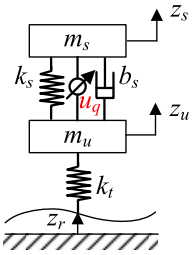

FIGURE 2. 2-DOF quarter-car model.

package, is conducted. The proposed VRFC is compared with conventional approaches, i.e., LQR, LQ SOF and LQ preview controllers, via simulation in terms of ride comfort.

The main contributions of this study are summarized as follows:

1) For active suspension control, the virtual reference is defined and the feedforward controller, the VRFC, is designed with the virtual reference. This type of virtual reference has not been proposed to date.
2) A simulation-based optimization is formulated to find optimum parameters of the VRFC and solved by a heuristic optimization method.
3) To use the VRFC in actual vehicles, the speed variation of a vehicle is considered and VRFC is optimized over speed variation.

This paper is composed of four sections. In Section II, LQR, LQ SOF and preview controllers for an active suspension system are designed with 2-DOF quarter-car model. VRFC is defined and optimized in Section III. In Section IV, A simulation with a vehicle dynamics simulation program is performed to evaluate the proposed controllers, and simulation results are analyzed and compared with one another. The conclusions are given in Section V.

II. DESIGN OF FEEDBACK AND PREVIEW CONTROLLERS FOR ACTIVE SUSPENSION

A. LQR DESIGN WITH A QUARTER-CAR MODEL

The configuration of a 2-DOF quarter-car model is depicted in Fig. 2. The vehicle body is modeled as sprung and unsprung masses to describe the vertical motions. This model assumes that the spring and damper are linear. For spring, it is assumed that a helical spring is used in the suspension. The force caused by the spring is linear with respect to the suspension stroke because it is associated not with the bending but with the torsion in the wire [37]. For damper, a viscous damping, i.e., linear damping is assumed. Viscous damping is valid when the fluid flow is relatively slow, i.e., laminar [38]. So, the suspension force f with control input u is calculated as (1). Based on the suspension force f, the equations of motion of the sprung and unsprung masses are derived as (2). By replacing f of (2) with that of (1) and rearranging it, the vector-matrix form of (2) is obtained as (3). After defining the vectors and matrices as given in (4), (3) is converted into (5). By defining the state vector as (6), the state-space equation for the 2-DOF quarter-car model is derived as (7) [33]. In (7), the system and input matrices are obtained as (8) from (4).

$$f = -k_s(z_s - z_u) - b_s(\dot{z}_s - \dot{z}_u) + u \tag{1}$$

$$\begin{cases} m_s\ddot{z}_s = f \\ m_u\ddot{z}_u = -f - k_t(z_u - z_r) \end{cases} \tag{2}$$

$$\begin{bmatrix} m_s & 0 \\ 0 & m_u \end{bmatrix}\begin{bmatrix} \ddot{z}_s \\ \ddot{z}_u \end{bmatrix} = \begin{bmatrix} -k_s & k_s \\ k_s & -k_s - k_t \end{bmatrix}\begin{bmatrix} z_s \\ z_u \end{bmatrix} + \begin{bmatrix} -b_s & b_s \\ b_s & -b_s \end{bmatrix}\begin{bmatrix} \dot{z}_s \\ \dot{z}_u \end{bmatrix} + \begin{bmatrix} 1 \\ -1 \end{bmatrix}u + \begin{bmatrix} 0 \\ k_t \end{bmatrix}z_r \tag{3}$$

$$\begin{cases} \mathbf{p} \triangleq \begin{bmatrix} z_s \\ z_u \end{bmatrix}, \quad \mathbf{q} \triangleq \begin{bmatrix} 1 \\ -1 \end{bmatrix}, \quad \mathbf{d} \triangleq \begin{bmatrix} 0 \\ k_t \end{bmatrix}, \\ \mathbf{M} \triangleq \begin{bmatrix} m_s & 0 \\ 0 & m_u \end{bmatrix}, \quad \mathbf{F} \triangleq \begin{bmatrix} -k_s & k_s \\ k_s & -k_s - k_t \end{bmatrix}, \\ \mathbf{B} \triangleq \begin{bmatrix} -b_s & b_s \\ b_s & -b_s \end{bmatrix} \end{cases} \tag{4}$$

$$\mathbf{M}\ddot{\mathbf{p}} = \mathbf{F}\mathbf{p} + \mathbf{B}\dot{\mathbf{p}} + \mathbf{d}z_r + \mathbf{q}u \tag{5}$$

$$\mathbf{x} = \begin{bmatrix} \mathbf{p} \\ \dot{\mathbf{p}} \end{bmatrix} = \begin{bmatrix} z_s & z_u & \dot{z}_s & \dot{z}_u \end{bmatrix}^T \tag{6}$$

$$\dot{\mathbf{x}} = \mathbf{A}\mathbf{x} + \mathbf{B}_1 z_r + \mathbf{B}_2 u \tag{7}$$

$$\mathbf{A} \triangleq \begin{bmatrix} \mathbf{0}_{2\times2} & \mathbf{I}_{2\times2} \\ \mathbf{M}^{-1}\mathbf{F} & \mathbf{M}^{-1}\mathbf{B} \end{bmatrix}, \quad \mathbf{B}_1 \begin{bmatrix} \mathbf{0}_{2\times1} \\ \mathbf{M}^{-1}\mathbf{d} \end{bmatrix}, \quad \mathbf{B}_2 \begin{bmatrix} \mathbf{0}_{2\times1} \\ \mathbf{M}^{-1}\mathbf{q} \end{bmatrix} \tag{8}$$

Based on the state vector of the quarter-car model, the LQ objective function J for LQR is defined as (9). The weight ρ_i is used to adjust the effect of each term in J to control gain. The value of ρ_i is determined by Bryson's rule given in (10) [39]. In (10), the maximum allowable value η is defined to determine ρ_i on the corresponding term in J. Under the condition that all weights are fixed, η_1 for the first term of J, the vertical acceleration of the sprung mass, should be set to a lower value. Meanwhile, to improve the road holding, η_3 for the tire deflection should have a higher value. After reorganizing J with the state vector (6), the weighting matrices, $\mathbf{Q}$, $\mathbf{N}$, and $\mathbf{R}$, can be derived as given (9). LQR, a full-state feedback controller, is used with the gain matrix $\boldsymbol{K}$, which is determined by the Riccati equation. Riccati equation is defined with $\mathbf{A}$, $\mathbf{B}_2$, $\mathbf{Q}$, $\mathbf{N}$, and $\mathbf{R}$. In this paper, the controller with $\mathbf{K}$ is denoted as LQRq.

$$J = \int_0^\infty \left\{\rho_1\ddot{z}_s^2 + \rho_2(z_s - z_u)^2 + \rho_3 z_u^2 + \rho_4 u^2\right\} dt = \int_0^\infty \left\{\begin{bmatrix} \mathbf{x} \\ u \end{bmatrix}^T \begin{bmatrix} \mathbf{Q} & \mathbf{N} \\ \mathbf{N}^T & \mathbf{R} \end{bmatrix}\begin{bmatrix} \mathbf{x} \\ u \end{bmatrix}\right\} dt \tag{9}$$

$$\rho_i = 1/\eta_i^2, \; i = 1, 2, 3, 4 \tag{10}$$

$$u = u_{fb} = -\mathbf{K}\mathbf{x} \tag{11}$$

In the previous literature, LQRq was designed for a full-car model under the assumption that a full-car model can be composed of four quarter-car models [33,34]. The controller derived from LQRq for the full-car model was called LQRfq. As shown in (6) and (11), LQRq and LQRfq do not need roll and pitch angles of a sprung mass for feedback control. However, it was shown that LQRq and LQRfq improved the roll and pitch motions of a sprung mass without measuring the roll and pitch angles of a sprung mass [34].

B. DESIGN OF LQR AND LQ CONTROLLER WITH A QUARTER-CAR MODEL

When implementing LQR based suspension controller with the quarter-car model, the precise measurement of the state variables of (6) is required to achieve the intended control performance. However, it is difficult to directly measure the height and velocity of the sprung and unsprung masses. To cope with the problem, it is desirable to use SOF control with available sensor signals [40], [41]. Therefore, SOF control has been adopted for the controller design of the active suspension system [42], [43]. In real vehicles, the vertical acceleration of the sprung mass and the suspension stroke are typically available. These signals have been used for semi-active suspension control [44]–[48]. In the previous work, it is assumed that the suspension stroke and its derivative are available to determine the control inputs [34]. This paper follows the assumption.

The SOF controller is defined as (12). Since the suspension stroke and its derivative are available for SOF control, the vector of sensor outputs is defined as $\mathbf{y}$ as given in (13) from the output matrix $\mathbf{C}$ and the state vector of (6). Because there are two sensor outputs, the dimension of the gain matrix, $\mathbf{K}_{SOF}$, is two by one. By replacing $\mathbf{y}$ in (12) with $\mathbf{Cx}$, the control input of SOF controller, u_{SOF}, is obtained as the full-state feedback form of (14). From (14), $\mathbf{Z}$ is the full-state feedback gain matrix of u_{SOF}.

$$u_{SOF} = \mathbf{K}_{SOF}\mathbf{y} \tag{12}$$

$$\mathbf{y} = \begin{bmatrix} z_s - z_u \\ \dot{z}_s - \dot{z}_u \end{bmatrix} = \begin{bmatrix} 1 & -1 & 0 & 0 \\ 0 & 0 & 1 & -1 \end{bmatrix} \mathbf{x} = \mathbf{Cx} \tag{13}$$

$$u_{SOF} = \mathbf{K}_{SOF}\mathbf{y} = \mathbf{K}_{SOF}\mathbf{Cx} = \mathbf{Zx} \tag{14}$$

Optimization problem is formulated to design LQ SOF controller. The optimization problem, (15), is solved to find $\mathbf{K}_{SOF}$ by minimizing the J in (9). In (15), the optimization variables are two elements of $\mathbf{K}_{SOF}$. Since the optimization problem for LQ SOF is non-convex and $\mathbf{Z}$ is structured, it has been known that there have been no methods, which guarantee to find a global optimum or a stable initial solution [40], [41].

$$\min_{\mathbf{K}_{SOF}} \quad J = \frac{1}{2}\text{trace}\left(\mathbf{P}\right), \mathbf{P} = \mathbf{P}^T > 0$$
$$s.t. \quad \begin{cases} \max\left(Re\left[\mathbf{A} + \mathbf{B}_2\mathbf{Z}\right]\right) < 0 \\ \left(\mathbf{A} + \mathbf{B}_2\mathbf{Z}\right)^T\mathbf{P} + \mathbf{P}\left(\mathbf{A} + \mathbf{B}_2\mathbf{Z}\right) \\ +\mathbf{Q} + \mathbf{Z}^T\mathbf{N}^T + \mathbf{NZ} + \mathbf{Z}^T\mathbf{RZ} = 0 \end{cases} \tag{15}$$

In this paper, the heuristic optimization method, CMA-ES, is applied to determine the optimum gain matrix $\mathbf{K}_{SOF}$ [49]. A detailed description of the optimization procedure with CMA-ES can be found in the previous work [34]. Let denote the LQ SOF controller, $\mathbf{K}_{SOF}$, which is obtained by solving (15), as LQSOFq. As mentioned earlier, LQSOFq was applied to a full-car model under the assumption that a full-car model can be represented by four quarter-car models [33], [34].

C. DESIGN OF LQ OPTIMAL PREVIEW CONTROLLER WITH A QUARTER-CAR MODEL

In general, LQ optimal preview control has been designed in the discrete-time domain. For the reason, the continuous-time state-space equation (7) is converted to the discrete-time one (16) by the discretization (17). In (17), T_s is the sampling time or rate of the discrete-time system.

$$\mathbf{x}\left(k+1\right) = \Phi\mathbf{x}\left(k\right) + \Pi z_r\left(k\right) + \Omega u\left(k\right) \tag{16}$$

$$\begin{cases} \Sigma\left(\sigma\right) = e^{\mathbf{A}\sigma} \\ \mathbf{\Phi} = \Sigma\left(T_s\right) \simeq \mathbf{I} + \mathbf{A}T_s \\ \Pi = \left\{\int_0^{T_s} \Sigma\left(\tau\right) d\tau\right\} \mathbf{B}_1 \simeq \mathbf{B}_1 T_s \\ \Omega = \left\{\int_0^{T_s} \Sigma\left(\tau\right) d\tau\right\} \mathbf{B}_2 \simeq \mathbf{B}_2 T_s \end{cases} \tag{17}$$

Let the preview period T_p be a multiple of the sampling period T_s, i.e., $p \cdot T_s$. Let $\mathbf{w}(k)$ be the vector containing all the preview signals within the preview period at instant k, as given in (18). With the definition of (18), the state-space equation of the vector $\mathbf{w}(k)$ is expressed as (19).

$$\mathbf{w}\left(k\right) = \left[z_r\left(k\right)\ z_r\left(k+1\right) \cdots z_r\left(k+p\right)\right]^T \tag{18}$$

$$\begin{aligned} \mathbf{w}\left(k+1\right) &= \begin{bmatrix} 0 & 1 & 0 & \cdots & 0 \\ 0 & 0 & 1 & \cdots & 0 \\ \vdots & \vdots & \vdots & \ddots & \vdots \\ 0 & 0 & 0 & \ddots & 1 \\ 0 & 0 & 0 & \cdots & 0 \end{bmatrix} \mathbf{w}\left(k\right) \\ &\quad + \begin{bmatrix} 0 \\ 0 \\ \vdots \\ 0 \\ 1 \end{bmatrix} z_r\left(k+p+1\right) \\ &= \mathbf{\Psi}\mathbf{w}\left(k\right) + \mathbf{\Xi} z_r\left(k+p+1\right) \end{aligned} \tag{19}$$

By augmenting (19) with (16), the augmented state-space equation of state and disturbance is obtained as (20) [7,14,18]. From (20), new matrices are defined as (21). With the vector and matrices of (21), (20) is rewritten as the state-space equation of (22).

$$\begin{bmatrix} \mathbf{x}\left(k+1\right) \\ \mathbf{w}\left(k+1\right) \end{bmatrix} = \begin{bmatrix} \mathbf{\Phi} & \mathbf{\Theta} \\ \mathbf{0} & \mathbf{\Psi} \end{bmatrix} \begin{bmatrix} \mathbf{x}\left(k\right) \\ \mathbf{w}\left(k\right) \end{bmatrix}$$

$$+\begin{bmatrix}\mathbf{0}\\ \mathbf{\Xi}\end{bmatrix} z_r\,(k+p+1)+\begin{bmatrix}\Omega\\ \mathbf{0}\end{bmatrix} u\,(k)$$

$$\mathbf{\Theta} \triangleq \begin{bmatrix}\Pi\ \mathbf{0}\ \cdots\ \mathbf{0}\end{bmatrix} \tag{20}$$

$$\bar{\mathbf{x}}\,(k) \triangleq \begin{bmatrix}\mathbf{x}\,(k)\\ \mathbf{w}\,(k)\end{bmatrix},\ \bar{\mathbf{A}} \triangleq \begin{bmatrix}\mathbf{\Phi}\ \mathbf{\Theta}\\ \mathbf{0}\ \ \mathbf{\Psi}\end{bmatrix},\ \bar{\mathbf{B}}_1 \triangleq \begin{bmatrix}\mathbf{0}\\ \mathbf{\Xi}\end{bmatrix},$$

$$\bar{\mathbf{B}}_2 \triangleq \begin{bmatrix}\Omega\\ \mathbf{0}\end{bmatrix} \tag{21}$$

$$\bar{\mathbf{x}}\,(k+1) = \bar{\mathbf{A}}\bar{\mathbf{x}}\,(k) + \bar{\mathbf{B}}_1\mathbf{w}\,(k+p+1) + \bar{\mathbf{B}}_2\mathbf{u}\,(k) \tag{22}$$

With the matrices $\mathbf{Q}$, $\mathbf{N}$ and $\mathbf{R}$ in (9), the new matrices for the augmented system are defined as (23). With those matrices and the augmented system (22), the LQ objective function (9) is also augmented with the previewed disturbances as (24).

$$\bar{\mathbf{Q}} \triangleq \begin{bmatrix}\mathbf{Q}\ \mathbf{0}\\ \mathbf{0}\ \ \mathbf{0}\end{bmatrix},\ \bar{\mathbf{N}} \triangleq \begin{bmatrix}\mathbf{N}\\ \mathbf{0}\end{bmatrix},\ \bar{\mathbf{R}} \triangleq \mathbf{R} \tag{23}$$

$$\bar{J} = \sum_{k=1}^{\infty}\begin{bmatrix}\bar{\mathbf{x}}^T\,(k)\,\bar{\mathbf{Q}}\bar{\mathbf{x}}\,(k) + u\,(k)\,\bar{\mathbf{N}}^T\bar{\mathbf{x}}\,(k)\\ +\bar{\mathbf{x}}^T\,(k)\,\bar{\mathbf{N}}u\,(k) + u\,(k)\,\bar{\mathbf{R}}u\,(k)\end{bmatrix} \tag{24}$$

The discrete-time LQ optimal preview controller is obtained as (25) from LQR for the augmented system (22) with LQ objective function (24). As shown in (25), LQR for the augmented system has the form of the full-state feedback control, which consists of the feedback and feedforward parts, $\mathbf{K}_{FB}$ and $\mathbf{K}_{FF}$, corresponding to the vectors of state and disturbance, respectively. In (25), $\mathbf{K}_{FB}$ is identical to $\mathbf{K}$ in (11).

$$u\,(k) = \bar{\mathbf{K}}\bar{\mathbf{x}}\,(k) = -\begin{bmatrix}\mathbf{K}_{FB}\ \mathbf{K}_{FF}\end{bmatrix}\begin{bmatrix}\mathbf{x}\,(k)\\ \mathbf{w}\,(k)\end{bmatrix} \tag{25}$$

The future road profile should be measured for preview control, as shown in (18). Moreover, those signals should be interpolated according to speed variation of a vehicle [50]. This interpolation should be done even though the signals are given via V2V communication from other vehicles. The virtual reference proposed in this paper does not need the future road profile or the shape of a bump because it requires only the center position of a real bump.

III. DESIGN OF VIRTUAL REFERENCE FEEDFORWARD CONTROLLERS FOR ACTIVE SUSPENSION

A. DESIGN OF A VIRTUAL REFERENCE FEEDFORWARD CONTROLLER

A virtual reference feedforward controller (VRFC) is defined as (26). In (26), $z_{s,ref}$ is a virtual reference on the vertical height of the sprung mass, used for VRFC and k_{ff} is the feedforward gain. This is virtual because $z_{s,ref}$ has no physical meaning. In other words, it is assumed that a real bump has the shape of a normal distribution regardless of a true shape of a bump, in this paper. The virtual reference $z_{s,ref}$ is defined as (27). This is an exponential function used to represent a normal distribution in statistics, as shown in Fig. 3. In Fig. 3, the legend Bump represents a real bump through where a vehicle passes. As shown in In (27), the virtual reference is a function of travel distance, x. In (27) and Fig. 3, h is a parameter used to tune the height of the virtual reference. μ and σ are the mean and standard deviation of the normal distribution, which are used to tune the center position and width of the virtual reference, respectively.

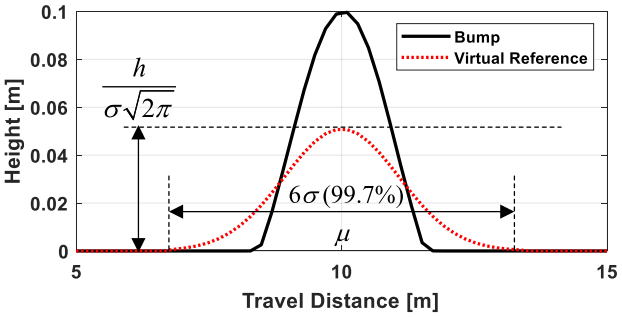

FIGURE 3. Actual and virtual reference bump profiles.

In this paper, the center position of the virtual reference, μ, is set to that of the real bump. In other words, this is set to the contact point of the tire and the road surface in the quarter-car model. This needs information on the location and height of a real bump. Hence, it is assumed that the location and height of a real bump are known a priori. Three parameters, i.e., k_{ff}, h, and σ, are needed to describe the virtual reference. These parameters should be determined to maximize the control performance of the VRFC. In (27), the parameter h is bounded as (28) in such a way that it is limited to the height of the bump, i.e., 0.1 in Fig. 3. By summing (11), (14) (26), the control inputs of LQRq and LQSOFq are calculated as (29) and (30), respectively.

$$u_{ff} = -k_{ff}\left(z_{s,ref} - z_s\right) \tag{26}$$

$$z_{s,ref}\,(x) = \frac{h}{\sigma\sqrt{2\pi}}\exp\left(-\frac{1}{2}\left(\frac{x-\mu}{\sigma}\right)^2\right) \tag{27}$$

$$0.0 \le h \le 0.1 \tag{28}$$

$$u_q = u_{fb} + u_{ff} = -\mathbf{K}\mathbf{x} - k_{ff}\left(z_{s,ref} - z_s\right) \tag{29}$$

$$u = u_{SOF} + u_{ff} = \mathbf{K}_{SOF}\mathbf{y} - k_{ff}\left(z_{s,ref} - z_s\right) \tag{30}$$

When optimizing (27), the first thing to do is to define an objective function. Generally, the objective of active suspension control is to improve ride comfort or reduce the vertical acceleration of the sprung mass. For the purpose, there are several types of objective functions. The first type is to use the LQ objective function, (9). This can be approximated as (31) by discretizing (7). The second type is to use (32). The third type is to use the maximum of the absolute vertical acceleration, i.e., (33). The next step for the optimization is to set a feedback controller used with the VRFC. There are two options: LQRq and LQSOFq as given in (29) and (30). After the objective function and the feedback controller are selected, the optimization is started.

The optimization variables are k_{ff}, h, and σ in (27). This problem is non-linear and non-convex. Hence, there are no analytic methods to find an optimum [51]. For the reason, a heuristic optimization method is adopted. In this paper, MATLAB built-in function, fminsearch(), is used for optimization. This command is an implementation of

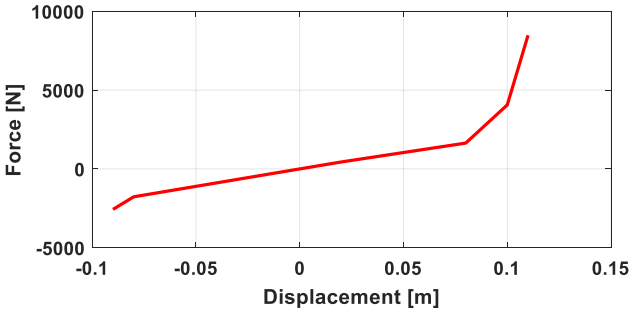

FIGURE 4. Spring stiffness curve of the quarter-car model.

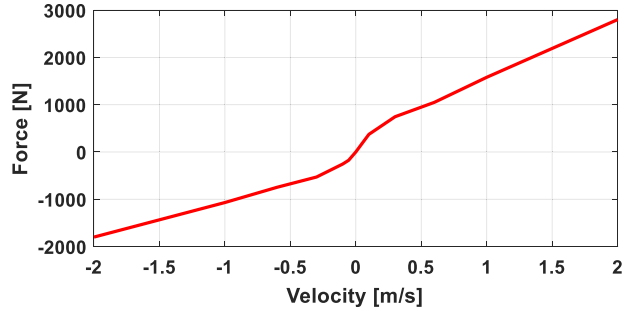

FIGURE 5. Damping coefficient curve of the quarter-car model.

Nelder-Mead simplex algorithm. The quarter-car model, (7), with the controller (29) or (30) is implemented with MATLAB/Simulink. In the Simulink code, the spring stiffness and the damping coefficient are replaced with the nonlinear curves, as given by Figs. 4 and 5, respectively. These were referred from Demo_Lexus_NX300h, which is the built-in vehicle model in CarMaker. Once the optimization variables are set to particular values, MATLAB/Simulink code is run by MATLAB command sim() and the variables in the objective functions are obtained from the Simulink code. Then, the objective functions, (31), (32) and (33), are calculated with the variables. Fig. 6 illustrates this procedure. Let denote the controllers of (29) with the VRFC optimized for (31), (32) and (33) as LQRqv1, LQRqv2, and LQRqv3, respectively. Let denote the controllers of (30) with the VRFC optimized for (31), (32) and (33) as LQSOFqv1, LQSOFqv2, and LQSOFqv3, respectively.

$$J_{q1} = \sum_{k=0}^{N} \left\{ \begin{array}{c} \rho_1 \ddot{z}_s^2(k) + \rho_2 \{z_s(k) - z_u(k)\}^2 \\ +\rho_3 z_u^2(k) + \rho_4 u_{fb}^2(k) \end{array} \right\} \quad (31)$$

$$J_{q2} = \sum_{k=0}^{N} \ddot{z}_s^2(k) \quad (32)$$

$$J_{q3} = \max |\ddot{z}_s(k)|, k = 0, 1, \cdots, N \quad (33)$$

B. DESIGN OF A VELOCITY-DEPENDENT VIRTUAL REFERENCE FEEDFORWARD CONTROLLER

The VRFC presented in the previous subsection was designed under the assumption that the vehicle speed is constant. However, this is not valid in actual driving conditions. To cope with the speed change, a new type VRFC is proposed.

New VRFC has constant h, and σ. The values of h and σ are set to 0.05 and 3.9279, respectively. Hence, there is only one parameter, k_{ff}, in (29) and (30), to be optimized. The vehicle speed is discretized from 10 km/h to 80 km/h with an interval of 10 km/h. For each speed, the feedforward gain, k_{ff} in VRFC, is optimized with the simulation-based optimization method. The parameters, h and σ, can be optimized over speed change. However, the virtual reference itself varies over speed change. This can distort the virtual reference profile. For the reason, it is assumed that h, and σ are constant.

The optimized feedforward gains are interpolated with respect to vehicle speed. With the data, the feedforward gain varies according to the vehicle speed. Let denote this VRFC as VRFFC.

TABLE 1. Parameter descriptions of its values of the 2-DOF quarter-car model.

m_q	487.5 kg	m_u	62.0 kg
k_s	45,000 N/m	b_s	3,500 N·s/m
k_t	391,961 N/m		

TABLE 2. Maximum allowable values in LQ objective function.

η_1	1.0 m/s^2	η_2	0.2 m	η_3	0.2 m
η_4	3,000 N				

IV. SIMULATION

In this section, the parameters of the virtual reference are optimized, and a simulation is conducted to verify the control performance of the designed VRFF on the vehicle simulation software, IPG CarMaker. IPG CarMaker has been widely used for validation on vehicle stability and active/semi-active suspension control over the last decade [52]–[55]. Through the simulation, the objective functions for the virtual reference are compared to one another.

Table 1 shows the descriptions and values of parameters for the quarter-car model. These values were referred from Demo_Lexus_NX300h, which is the built-in vehicle model in CarMaker and has characteristics of both internal combustion engine vehicles and electric vehicles. The weights in the LQ objective functions, (9), are calculated by (10) with the maximum allowable values given in Table 2. The weights used in this study focus on the improvement of ride comfort. In other words, the reduction of the vertical acceleration of the sprung mass is the primary goal of the proposed controller. As a consequence, the road adhesion will deteriorate. In this paper, it is assumed that the bandwidth of the actuator is infinite in generating an active control force and that there are no limits on the maximum force of the actuator.

A. OPTIMIZATION ON VIRTUAL REFERENCE FEEDFORWARD CONTROLLER

Three parameters of the virtual reference are optimized for three objective functions, (31), (32) and (33). As mentioned

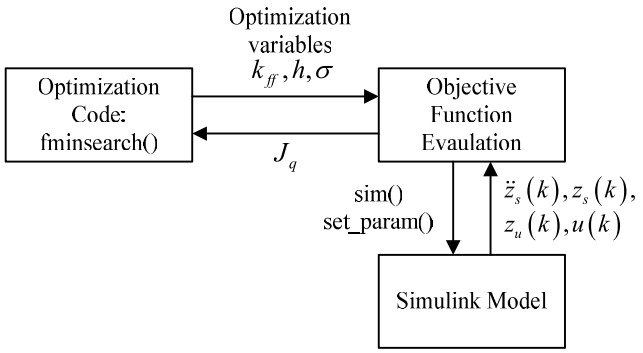

FIGURE 6. Procedure to calculate the optimization.

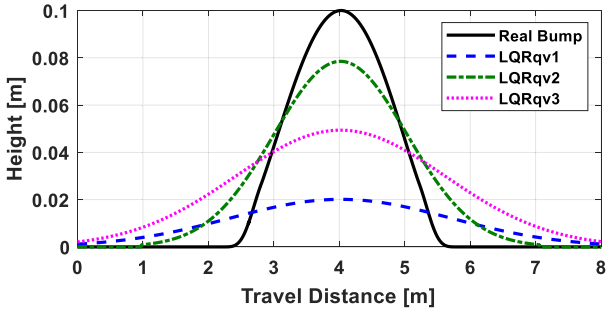

FIGURE 7. Optimized virtual reference profiles under LQRq.

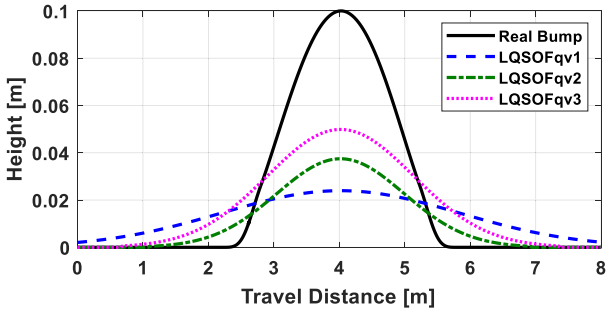

FIGURE 8. Optimized virtual reference profiles under LQSOFq.

earlier, this is done with MATLAB built-in function, fminsearch().

Figs. 7 and 8 show the virtual references optimized for the three objective functions with the feedback controllers, LQRq and LQSOFq, respectively. As mentioned earlier, the virtual reference is generated for the height of a sprung mass. Hence, it can be expected that the virtual reference near a real bump can give better performance than that far from one. As shown in Fig. 7, LQRqv2 nearly approaches the real bump. On the contrary, LQRqv1 is far from the real bump. Hence, it is expected that LQRqv2 and LQRqv1 give the best and worst performances in terms of ride comfort, respectively. The heights of the virtual reference optimized with LQSOFq as given in Fig. 8 are smaller than those optimized with LQRq as given in Fig. 7. Therefore, VRFC with LQRq is superior to one with LQSOFq.

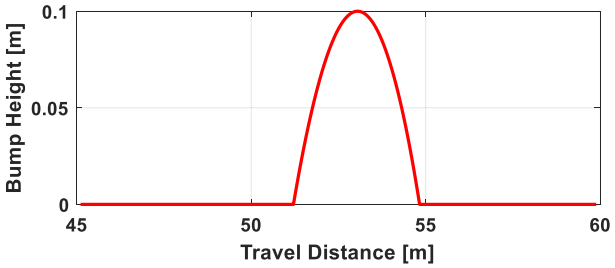

FIGURE 9. Single bump profile.

B. SIMULATION OF VRFC ON CARMAKER

The simulation for the designed VRFCs is conducted on the co-simulation environment with MATLAB/Simulink and the vehicle simulation package, IPG CarMaker. The simulation scenario is a single bump. Three sets of controllers are used for simulation. The first set consists of the passive system, LQRq, LQRqv1, LQRqv2 and LQRqv3. The second set consists of the passive system, LQSOFq, LQSOFqv1, LQSOFqv2 and LQSOFqv3. The third set consists of the passive system, LQRqv2, LQSOFqv2 and the preview controller presented in the subsection III.C.

The vehicle model is Demo_Lexus_NX300h, which is the built-in model of CarMaker. Fig. 9 shows the bump profile used for simulation, which has a length of 3.6 m and a height of 0.1 m. The initial condition of the vehicle is a stand-still position. Then, the vehicle accelerates to 30 km/h by a built-in speed controller in CarMaker. After reaching 30 km/h, the vehicle passes the bump. In the simulation, the tire-road friction coefficient is set to 0.8.

The simulation results of the first set of controllers are summarized in Fig. 10. As shown in Fig. 10, three controllers with VRFC are superior to LQRq in terms of ride comfort. This is expected from the fact that VRFCs are optimized after LQRq is designed. Among VRFCs, LQRqv2 shows the best performance in terms of ride comfort. Moreover, LQRqv2 and LQRqv3 show nearly identical performance in terms of ride comfort. This was expected from the results as given in Fig. 7. The difference between LQRqv2 and LQRqv3 is the magnitudes of the control inputs, as shown in Fig. 10-(e). The maximum control input of LQRqv3 is smaller than that of LQRqv2 while these shows the nearly same peaks of vertical accelerations. The most notable feature of VRFC is that the vertical acceleration and the suspension stroke were simultaneously reduced because these are conflicting with each other in general.

Fig. 11 shows the simulation results for the second set of the controllers, i.e., VRFCs with LQSOFq. As shown in Fig. 11, three controllers with VRFC are superior to LQSOFq in terms of ride comfort. This is expected from the fact that VRFCs are optimized after LQSOFq is designed. As shown in Fig. 11, LQSOFqv2 shows the best performance in terms of ride comfort. Different from the results in Fig. 7, LQSOFqv3 is superior to the other VRFCs in terms of other measures. Hence, it is desirable to use LQSOFqv2, i.e., LQSOFq with

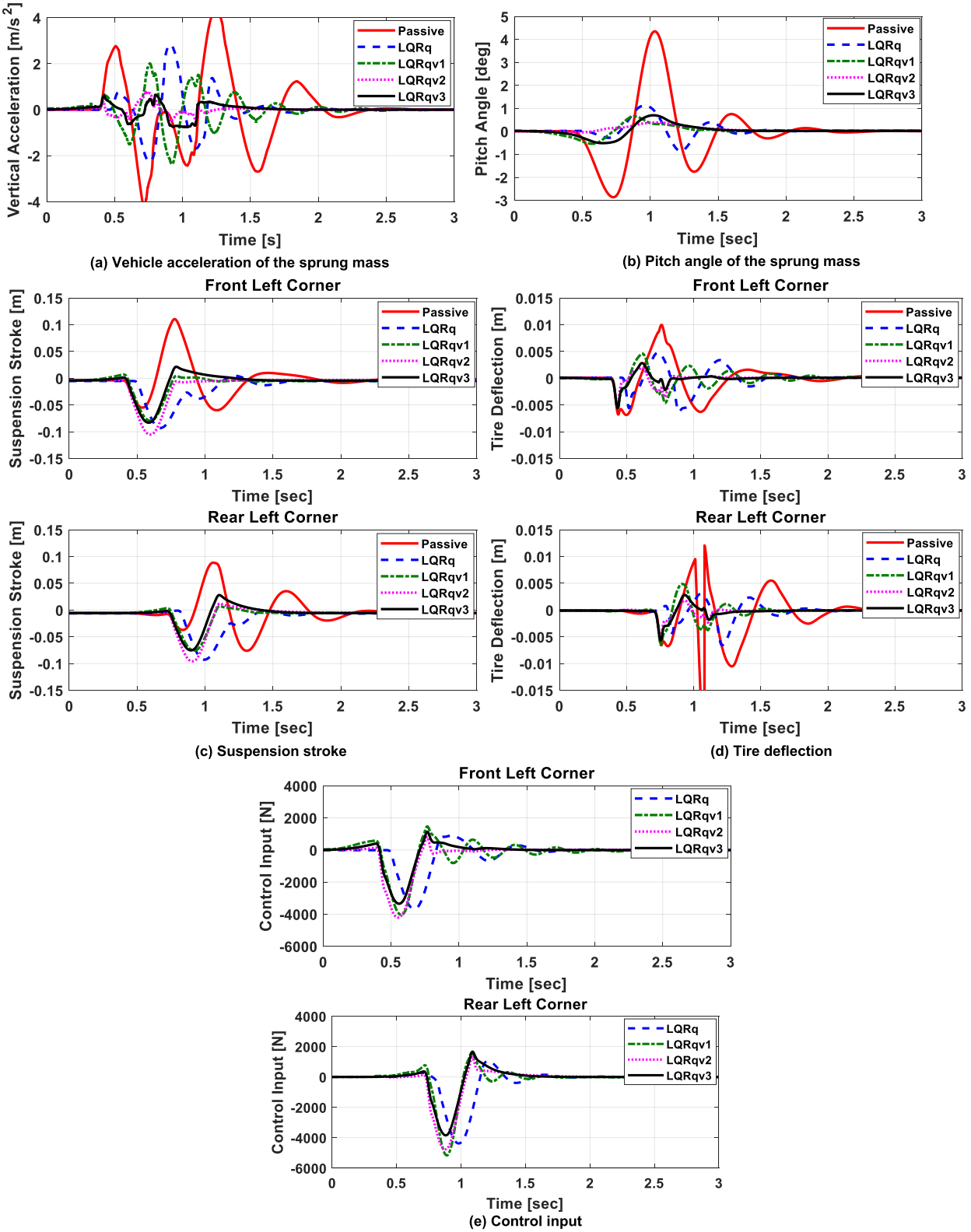

FIGURE 10. Simulation results obtained from CarMaker for each controller.

VRFC, for active suspension control. Different from the controllers, LQRqv2 and LQRqv3, the peak values of the control inputs and the suspension strokes of VRFCs with LQSOFq are nearly same to one another.

The simulation for the third set of controllers, i.e., the passive system, LQRqv2 and LQSOFv2, and LQ preview controller is conducted. For the LQ preview controller, the sampling time and the preview period were set to

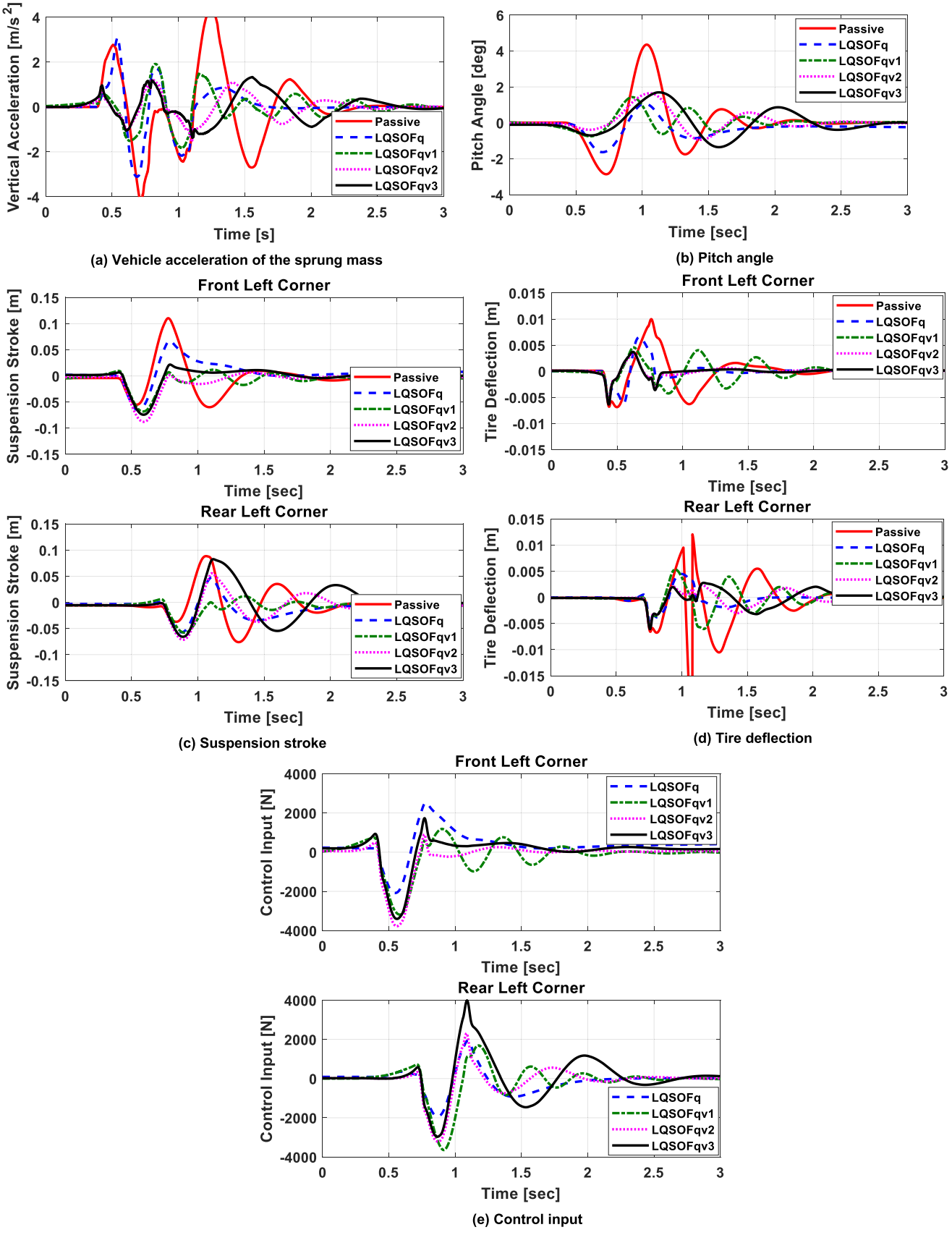

FIGURE 11. Simulation results obtained from CarMaker for each controller.

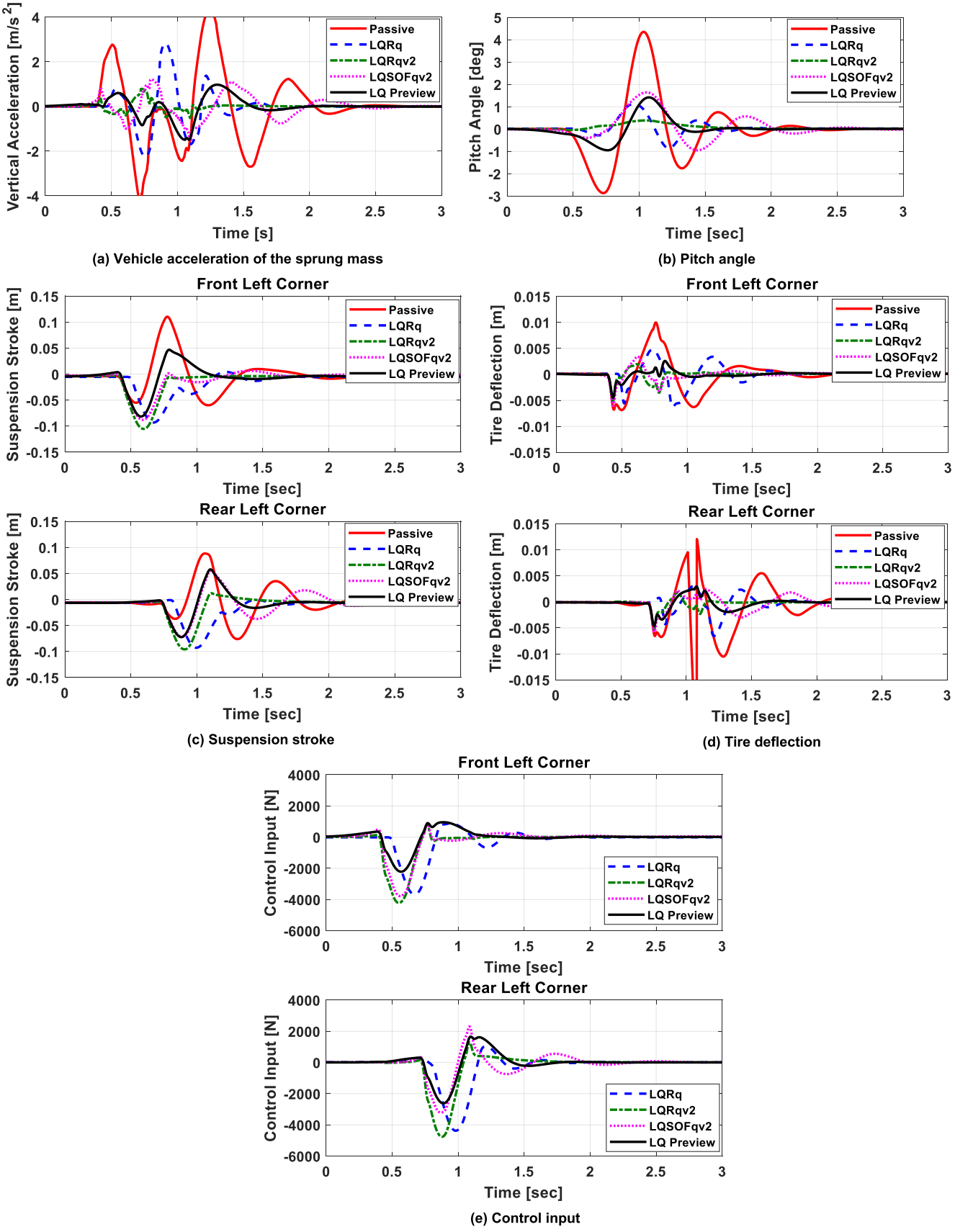

FIGURE 12. Simulation results obtained from CarMaker for each controller.

TABLE 3. Peak-to-peak values of responses for each controller at front left corner.

	$\ddot{z}_c$ (m/s^2)	θ (deg)	SS (m)	TD (m)	Control input (N)
Passive	8.6	7.2	0.170	0.017	0
LQRq	5.1	2.0	0.097	0.011	4557
LQRqv1	4.4	1.2	0.086	0.010	5506
LQRqv2	1.4	0.4	0.102	0.007	5025
LQRqv3	1.4	1.2	0.105	0.008	4481
LQSOFq	6.2	2.7	0.132	0.013	4606
LQSOFqv1	3.7	2.2	0.080	0.010	4380
LQSOFqv2	2.8	2.6	0.094	0.008	4674
LQSOFqv3	2.7	3.1	0.096	0.009	5138
LQ Preview	2.5	2.4	0.128	0.007	3172

TABLE 4. Percentage reduction of responses with respect to passive case for each controller at front left corner.

	$\ddot{z}_c$	θ	SS	TD
LQRq	59	27	57	64
LQRqv1	51	16	50	58
LQRqv2	16	5	60	41
LQRqv3	16	16	61	47
LQSOFq	72	37	77	76
LQSOFqv1	43	30	47	58
LQSOFqv2	32	36	55	47
LQSOFqv3	31	43	56	53
LQ Preview	29	33	75	41

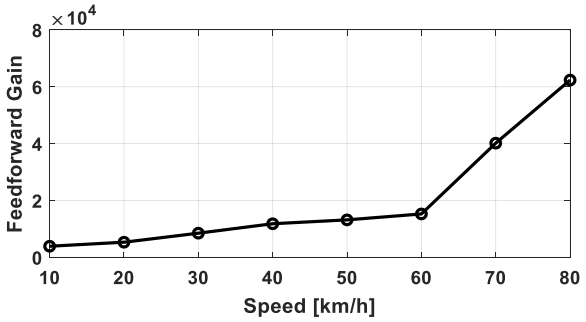

FIGURE 13. Variation of optimum preview gain with respect to vehicle speed

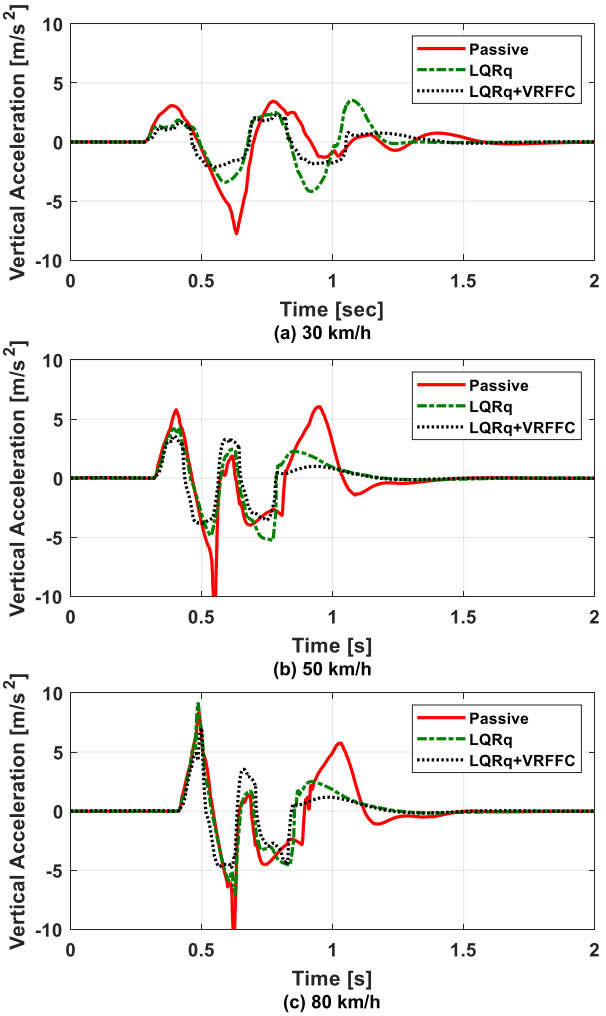

FIGURE 14. Vertical accelerations obtained from CarMaker for each vehicle speed on the single bump.

0.001sec and 0.1sec, respectively. Fig. 12 shows the simulation results for the third set of the controllers. As shown in Fig. 12-(a) and -(b), the VRFC, i.e., LQRqv2, is superior to the LQ preview controller in terms of ride comfort. LQSOFqv2 is comparable to the LQ preview controller. As shown in Fig. 12-(c) and -(d), the LQ preview controller gives larger positive suspension strokes and smaller tire deflections than the others. This is typical for the LQ controller designed with the full-car model. Hence, it is desirable to use the VRFC, LQRqv2, instead of the LQ preview controller for active suspension control.

Tables 3 shows the peak-to-peak values of the responses of the front left corner in Figs. 10, 11 and 12 for each controller, respectively. Table 4 shows the percentage reduction of the responses of the front left corner with respect to the passive case, calculated from Table 3. In these tables, the suspension stroke and the tire deflection are abbreviated to SS and TD, respectively. As shown in Tables 3 and 4, LQRqv2 and LQRqv3 give the smallest vertical acceleration than LQRq, LQRqv1 and the LQ preview controller. In other words, these controllers can provide the best performance in terms of ride comfort. For example as shown in Table 4, the vertical accelerations of LQRv2 and LQRv3 were reduced to 16% of the passive case and to 30% of LQRq. In terms of the pitch angle, LQRqv2 shows the best performance among controllers although it uses the largest control input. Compared to LQRq with VRFC, LQSOF controllers with VRFC shows poor performance in terms of all measures. In view of the feedforward control, LQRv2 is better than the LQ preview controller in terms of ride comfort. The vertical accelerations of LQRv2 and the LQ preview controller were

reduced to 16% and to 29% of the passive suspension. Hence, it is not recommended that VRFC is combined with LQSOFq although LQSOFq has only five gain elements. Moreover, it is recommended that VRFC is combined with LQRqv2.

C. SIMULATION OF VRFFC ON CARMAKER

The simulation with VRFFC described in the subsection III.B is done under the same condition as that of the subsection IV.B. VRFFC, i.e., the feedforward gain of VRFC, was designed with the fixed parameters, $h = 0.05$ and $\sigma = 3.9279$, which were obtained from the optimization on VRFC at 30 km/h.

Figs. 13 and 14 show the optimized feedforward gains and simulation results of VRFFC over speed change, respectively. As shown in Fig. 13, these gains significantly increase over 60 km/h. This is natural because the vehicle speed has a large effect on the vertical acceleration of the sprung mass. In fact, it is very hard for the active suspension to reduce the vertical acceleration of the sprung mass over 60 km/h due to actuator limitations on the maximum force, bandwidth, and moving velocity. For the reason, the control performance of VRFFC deteriorates as the vehicle speed increases over 60 km/h. This fact can be checked in Fig. 14. As shown in Fig. 14-(c), the active suspension controllers, LQRq and LQRq+VRFFC, have little effects on controlling the vertical acceleration of the sprung mass if the vehicle speed is over 80 km/h. On the contrary, VRFFC shows good performance in controlling the vertical acceleration of the sprung mass near 30 km/h.

V. CONCLUSION

In this paper, the virtual reference on heave motion of a sprung mass representing a bump was proposed for an active suspension system under the assumption that a real bump has the shape of a normal distribution regardless of a true shape of a bump. This virtual reference has the shape of normal distribution, whose two parameters are used to describe it. The feedforward controller with the form of P-control, called VRFC, was designed with the virtual reference. To maximize the performance for active suspension control, the two parameters of the virtual reference and feedforward gain were optimized with MATLAB/Simulink model and fminsearch() given in MATLAB. To cope with the speed variation of a vehicle, the feedforward gain was optimized with respect to a particular vehicle speed while the other parameters were fixed. With this manner, the feedforward gain varies according to the change in vehicle speed. To check the performance of the VRFC, the simulation on the vehicle simulation package, CarMaker, was conducted. From the simulation results, it was confirmed that the vertical acceleration of the VRFC designed with the quadratic objective function on it reduced to 16% of the passive case and to 30% of LQRq. Hence, in terms of ride comfort, it can be concluded that the VRFC designed with the quadratic objective function on the vertical acceleration is quite effective. It was also confirmed that the VRFC has little effect on ride comfort as the vehicle speed increases over 80 km/h. Further research can include the design of a tracking controller to make the height of the sprung mass follow the virtual reference.

REFERENCES

[1] D. Hrovat, "Survey of advanced suspension developments and related optimal control applications," *Automatica*, vol. 33, no. 10, pp. 1781–1817, 1997, doi: 10.1016/S0005-1098(97)00101-5.
[2] H. E. Tseng and D. Hrovat, "State of the art survey: Active and semi-active suspension control," *Vehicle Syst. Dyn.*, vol. 53, no. 7, pp. 1034–1062, 2015, doi: 10.1080/00423114.2015.1037313.
[3] *Mechanical Vibration and Shock Evaluation of Human Exposure to Whole-Body Vibration—Part 1: General Requirements*, Standard ISO 2631-1, International Organization for Standardization, Geneva, Switzerland, 1997.
[4] A. N. Rimell and N. J. Mansfield, "Design of digital filters for frequency weightings required for risk assessments of workers exposed to vibration," *Ind. Health*, vol. 45, no. 4, pp. 512–519, 2007, doi: 10.2486/indhealth.45.512.
[5] D. Cao, X. Song, and M. Ahmadian, "Editors' perspectives: Road vehicle suspension design, dynamics, and control," *Vehicle Syst. Dyn.*, vol. 49, nos. 1–2, pp. 3–28, Feb. 2011, doi: 10.1080/00423114.2010.532223.
[6] W. S. Aboud, S. M. Haris, and Y. Yaacob, "Advances in the control of mechatronic suspension systems," *J. Zhejiang Univ., Sci. C*, vol. 15, no. 10, pp. 848–860, 2014, doi: 10.1631/jzus.C14a0027.
[7] J. Theunissen, A. Tota, P. Gruber, M. Dhaens, and A. Sorniotti, "Preview-based techniques for vehicle suspension control: A state-of-the-art review," *Annu. Rev. Control*, vol. 51, pp. 206–235, Jan. 2021, doi: 10.1016/j.arcontrol.2021.03.010.
[8] T. Nguyen, "Application of optimization methods to controller design for active suspensions," Ph.D. dissertation, Dept. Chair Eng. Mech. Vehicle Dyn., German Res. Inst. Cottbus, Brandenburg Univ. Technol., Cottbus, Germany, 2006.
[9] M. Rahman and G. Rideout, "Using the lead vehicle as preview sensor in convoy vehicle active suspension control," *Vehicle Syst. Dyn.*, vol. 50, no. 12, pp. 1923–1948, 2012, doi: 10.1080/00423114.2012.707801.
[10] N. Birla and A. Swarup, "Optimal preview control: A review," *Optim. Control Appl. Methods*, vol. 36, no. 2, pp. 241–268, 2015, doi: 10.1002/oca.2106.
[11] A. Hac, "Optimal linear preview control of active vehicle suspension," *Vehicle Syst. Dyn.*, vol. 21, no. 1, pp. 167–195, Jan. 1992, doi: 10.1080/00423119208969008.
[12] M. B. A. Abdel-Hady, "Active suspension with preview control," *Vehicle Syst. Dyn.*, vol. 23, no. 1, pp. 1–13, Jan. 1994, doi: 10.1080/00423119308969500.
[13] T. J. Gordon, L. Palkovics, C. Pilbeam, and R. S. Sharp, "Second generation approaches to active and semi-active suspension control system design," *Vehicle Syst. Dyn.*, vol. 23, no. 1, pp. 158–171, Jan. 1994, doi: 10.1080/00423119308969512.
[14] S. M. EI-Demerdash and D. A. Crolla, "Hydro-pneumatic slow-active suspension with preview control," *Vehicle Syst. Dyn.*, vol. 25, no. 5, pp. 369–386, May 1996, doi: 10.1080/00423119608968972.
[15] A. G. Thompson and C. E. M. Pearce, "Performance index for a preview active suspension applied to a quarter-car model," *Vehicle Syst. Dyn.*, vol. 35, no. 1, pp. 55–66, Jan. 2001, doi: 10.1076/vesd.35.1.55.5616.
[16] M. El Madany, Z. Abduljabbar, and M. Foda, "Optimal preview control of active suspensions with integral constraint," *J. Vibrat. Control*, vol. 9, no. 12, pp. 1377–1400, Dec. 2003, doi: 10.1177/1077546304031167.
[17] B.-L. Zhang, G.-Y. Tang, and F.-L. Cao, "Optimal sliding mode control for active suspension systems," in *Proc. Int. Conf. Netw., Sens. Control*, Mar. 2009, pp. 351–356, doi: 10.1109/ICNSC.2009.4919300.
[18] S. De Bruyne, H. Van der Auweraer, J. Anthonis, W. Desmet, and J. Swevers, "Preview control of a constrained hydraulic active suspension system," in *Proc. IEEE 51st IEEE Conf. Decis. Control (CDC)*, Dec. 2012, pp. 4400–4405, doi: 10.1109/CDC.2012.6425847.
[19] S.-Y. Han, Y.-H. Chen, K. Ma, D. Wang, A. Abraham, and Z.-G. Liu, "Feedforward and feedback optimal vibration rejection for active suspension discrete-time systems under in-vehicle networks," in *Proc. 6th World Congr. Nature Biologically Inspired Comput. (NaBIC)*, Jul. 2014, pp. 139–144, doi: 10.1109/NaBIC.2014.6921868.
[20] C. Göhrle, A. Schindler, A. Wagner, and O. Sawodny, "Road profile estimation and preview control for low-bandwidth active suspension systems," *IEEE/ASME Trans. Mechatronics*, vol. 20, no. 5, pp. 2299–2310, Oct. 2015, doi: 10.1109/TMECH.2014.2375336.

[21] M. Sever and H. Yazici, "Disturbance observer based optimal controller design for active suspension systems," *IFAC-PapersOnLine*, vol. 49, no. 9, pp. 105–110, 2016, doi: 10.1016/j.ifacol.2016.07.505.

[22] J. Theunissen, A. Sorniotti, P. Gruber, S. Fallah, M. Ricco, M. Kvasnica, and M. Dhaens, "Regionless explicit model predictive control of active suspension systems with preview," *IEEE Trans. Ind. Electron.*, vol. 67, no. 6, pp. 4877–4888, Jun. 2020, doi: 10.1109/TIE.2019.2926056.

[23] J. Zhao, X. Wang, P. K. Wong, Z. Xie, J. Jia, and W. Li, "Multi-objective frequency domain-constrained static output feedback control for delayed active suspension systems with wheelbase preview information," *Nonlinear Dyn.*, vol. 103, no. 2, pp. 1757–1774, Jan. 2021, doi: 10.1007/s11071-021-06204-w.

[24] M. Papadimitrakis and A. Alexandridis, "Active vehicle suspension control using road preview model predictive control and radial basis function networks," *Appl. Soft Comput.*, vol. 120, May 2022, Art. no. 108646, doi: 10.1016/j.asoc.2022.108646.

[25] M. D. Donahue, "Implementation of an active suspension, preview controller for improved ride comfort," M.S. thesis, Dept. Mech. Eng., Univ. California, Berkeley, Berkeley, CA, USA, 2001.

[26] M. D. Donahue and J. K. Hedrick, "Implementation of an active Suspension. Preview controller for improved ride comfor," in *Nonlinear and Hybrid Systems in Automotive Control*. London, U.K.: Springer, 2003, pp. 1–22.

[27] A. Yamamoto, H. Sugai, R. Kanda, and S. Buma, "Preview ride comfort control for electric active suspension (eActive3)," SAE Tech. Paper 2014-01-0057, 2014, doi: 10.4271/2014-01-0057.

[28] S. Cytrynski, U. Neerpasch, R. Bellmann, and B. Danner, "The active suspension of the new mercedes-benz GLE," *ATZ Worldwide*, vol. 120, no. 12, pp. 42–45, Dec. 2018, doi: 10.1007/s38311-018-0172-y.

[29] *Wikipedia, Active Body Control*. Accessed: Apr. 4, 2022. [Online]. Available: https://en.wikipedia.org/wiki/Active_Body_Control

[30] V. S. K. P. Varma, S. Adarsh, K. I. Ramachandran, and B. B. Nair, "Real time detection of speed hump/bump and distance estimation with deep learning using GPU and ZED stereo camera," *Proc. Comput. Sci.*, vol. 143, pp. 988–997, Jan. 2018, doi: 10.1016/j.procs.2018.10.335.

[31] K. M. Lion, K. H. Kwong, and W. K. Lai, "Smart speed bump detection and estimation with Kinect," in *Proc. 4th Int. Conf. Control, Autom. Robot. (ICCAR)*, Apr. 2018, pp. 465–469, doi: 10.1109/ICCAR.2018.8384721.

[32] D. K. Dewangan and S. P. Sahu, "Deep learning-based speed bump detection model for intelligent vehicle system using raspberry pi," *IEEE Sensors J.*, vol. 21, no. 3, pp. 3570–3578, Feb. 2021, doi: 10.1109/JSEN.2020.3027097.

[33] M. Park and S. Yim, "Design of static output feedback and structured controllers for active suspension with quarter-car model," *Energies*, vol. 14, no. 24, p. 8231, Dec. 2021, doi: 10.3390/en14248231.

[34] Y. Jeong, Y. Sohn, S. Chang, and S. Yim, "Design of static output feedback controllers for an active suspension system," *IEEE Access*, vol. 10, pp. 26948–26964, 2022, doi: 10.1109/ACCESS.2022.3157326.

[35] Q.-G. Wang, Y. Zhang, and X.-G. Huang, "Virtual feedforward control for asymptotic rejection of periodic disturbance," *IEEE Trans. Ind. Electron.*, vol. 49, no. 3, pp. 566–573, Jun. 2002, doi: 10.1109/TIE.2002.1005381.

[36] Q.-G. Wang and H.-Q. Zhou, "Modified virtual feedforward control for periodic disturbance rejection," in *Proc. 4th Int. Conf. Control Autom. ICCA Final Program Book Abstr. (ICCA)*, Jun. 2003, pp. 203–207, doi: 10.1109/ICCA.2003.1595013.

[37] J. P. Bandstra, "Comparison of equivalent viscous damping and nonlinear damping in discrete and continuous vibrating systems," *J. Vibrat. Acoust.*, vol. 105, no. 3, pp. 382–392, Jul. 1983, doi: 10.1115/1.3269117.

[38] R. Champion and W. L. Champion, "Departure from linear mechanical behaviour of a helical spring," *Math. Comput. Model.*, vol. 53, nos. 5–6, pp. 915–926, Mar. 2011, doi: 10.1016/j.mcm.2010.10.028.

[39] A. E. Bryson and Y. Ho, *Applied Optimal Control*. New York, NY, USA: Taylor & Francis Group, 1975, p. 149.

[40] V. L. Syrmos, C. T. Abdallah, P. Dorato, and K. Grigoriadis, "Static output feedback-A survey," *Automatica*, vol. 33, no. 2, pp. 125–137, 1997, doi: 10.1016/S0005-1098(96)00141-0.

[41] M. S. Sadabadi and D. Peaucelle, "From static output feedback to structured robust static output feedback: A survey," *Annu. Rev. Control*, vol. 42, pp. 11–26, Jan. 2016, doi: 10.1016/j.arcontrol.2016.09.014.

[42] G. Wang, C. Chen, and S. Yu, "Optimization and static output-feedback control for half-car active suspensions with constrained information," *J. Sound Vibrat.*, vol. 378, pp. 1–13, Sep. 2016, doi: 10.1016/j.jsv.2016.05.033.

[43] J. Mrazgua, R. Chaibi, E. H. Tissir, and M. Ouahi, "Static output feedback stabilization of T-S fuzzy active suspension systems," *J. Terramech.*, vol. 97, pp. 19–27, Oct. 2021, doi: 10.1016/j.jterra.2021.05.001.

[44] M. Fleps-Dezasse, M. M. Ahmed, J. Brembeck, and F. Svaricek, "Experimental evaluation of linear parameter-varying semi-active suspension control," in *Proc. IEEE Conf. Control Appl. (CCA)*, Sep. 2016, pp. 77–84, doi: 10.1109/CCA.2016.7587825.

[45] Y. Qin, C. Xiang, Z. Wang, and M. Dong, "Road excitation classification for semi-active suspension system based on system response," *J. Vibrat. Control*, vol. 24, no. 13, pp. 2732–2748, Jul. 2018, doi: 10.1177/1077546317693432.

[46] M. M. Morato, M. Q. Nguyen, O. Sename, and L. Dugard, "Design of a fast real-time LPV model predictive control system for semi-active suspension control of a full vehicle," *J. Franklin Inst.*, vol. 356, no. 3, pp. 1196–1224, Feb. 2019, doi: 10.1016/j.jfranklin.2018.11.016.

[47] Y. Liu and L. Zuo, "Mixed skyhook and power-driven-damper: A new low-jerk semi-active suspension control based on power flow analysis," *J. Dyn. Syst., Meas., Control*, vol. 138, no. 8, Aug. 2016, Art. no. 081009, doi: 10.1115/1.4033073.

[48] A. Soliman and M. Kaldas, "Semi-active suspension systems from research to mass-market—A review," *J. Low Freq. Noise, Vibrat. Act. Control*, vol. 40, no. 2, pp. 1005–1023, Jun. 2021, doi: 10.1177/1461348419876392.

[49] N. Hansen, S. D. Müller, and P. Koumoutsakos, "Reducing the time complexity of the derandomized evolution strategy with covariance matrix adaptation (CMA-ES)," *Evol. Comput.*, vol. 11, no. 1, pp. 1–18, Mar. 2003, doi: 10.1162/106365603321828970.

[50] J. Nah and S. Yim, "Observer-based active roll preview control with V2V communication," *IEEE Access*, vol. 7, pp. 44831–44839, 2019, doi: 10.1109/ACCESS.2019.2909049.

[51] V. Landersheim, M. Jurisch, R. Bartolozzi, G. Stoll, R. Möller, and H. Atzrodt, "Simulation-based testing of subsystems for autonomous vehicles at the example of an active suspension control system," *Electronics*, vol. 11, no. 9, p. 1469, May 2022, doi: 10.3390/electronics11091469.

[52] D. Quaini, K. Sazgetdinov, V. Ivanov, and A. Ferrara, "Optimization based sliding mode control in active suspensions: Design and hardware-in-the-loop assessment," in *Proc. Eur. Control Conf. (ECC)*, May 2020, pp. 1607–1612, doi: 10.23919/ECC51009.2020.9143835.

[53] G. Papaioannou, J. Jerrelind, and L. Drugge, "A study on skyhook-based suspension control algorithms with regards to tyre wear minimisation in hybrid vehicles," in *Proc. IEEE Int. Intell. Transp. Syst. Conf. (ITSC)*, Sep. 2021, pp. 19–22, doi: 10.1109/ITSC48978.2021.9564409.

[54] D. Fényes, M. Fazekas, B. Németh, and P. Gáspár, "Implementation of a variable-geometry suspension-based steering control system," *Vehicle Syst. Dyn.*, vol. 60, no. 6, pp. 2018–2035, Jun. 2022, doi: 10.1080/00423114.2021.1890798.

[55] X. Hou, J. Zhang, Y. Ji, W. Liu, and C. He, "Autonomous drift controller for distributed drive electric vehicle with input coupling and uncertain disturbance," *ISA Trans.*, vol. 120, pp. 1–17, Jan. 2022, doi: 10.1016/j.isatra.2021.03.009.

YONGHWAN JEONG received the B.S. and Ph.D. degrees in mechanical engineering from Seoul National University, South Korea, in 2014 and 2020, respectively. From 2020 to 2021, he was a Senior Research Engineer with Hyundai Motor Company, South Korea. Since 2021, he has been an Assistant Professor with the Department of Mechanical and Automotive Engineering, Seoul National University of Science and Technology, South Korea. His research interests include sensor fusion with vehicular communication, risk assessment, driver intention inference with trajectory prediction, and motion planning and control of urban automated vehicle.

YOUNGIL SOHN received the B.S. and M.S. degrees in mechanical engineering from the Korea Advanced Institute of Science and Technology (KAIST), South Korea, in 1994 and 1996, respectively. From 1996 to 2012, he was a Principal Research Engineer with the Institute for Advanced Engineering (IAE), South Korea. From 2012 to 2021, he was a Senior Research Engineer with the Research and Development Center, Hyundai Motor Company. Since 2021, he has been working as a Senior Research Engineer with the Institute of Advanced Technology Development (IATD), Hyundai Motor Company, South Korea. His research interests include control software development for semi-active and active suspension for vehicle ride comfort and artificial intelligent application for vehicle chassis control.

SEHYUN CHANG received the B.S. degree from Korea Aerospace University, South Korea, in 1996, the M.S. degree in aeronautical engineering from Seoul National University, South Korea, in 1998, and the Ph.D. degree in mechanical engineering from the University of Michigan, Ann Arbor, in 2007. Since 2007, he has been a Senior Research Engineer with the Research and Development Center, Hyundai Motor Company, South Korea. His research interests include vehicle dynamics, integrated chassis control, model predictive control, future mobility, and design optimization,

SEONGJIN YIM (Member, IEEE) received the B.S. degree in mechanical engineering from Yonsei University, South Korea, in 1995, and the M.S. and Ph.D. degrees in mechanical engineering from the Korea Advanced Institute of Science and Technology (KAIST), in 1997 and 2007, respectively.

From 2008 to 2010, he was a Postdoctoral Researcher with the BK21 School for Creative Engineering Design of Next Generation Mechanical and Aerospace Systems, Seoul National University. From 2011 to 2013, he was a Research Professor with the Advanced Institutes of Convergence Technology, Seoul National University. Since 2019, he has been an Associate Professor with the Department of Mechanical and Automotive Engineering, Seoul National University of Science and Technology, South Korea. His research interests include autonomous driving, integrated chassis control systems with V2V communication, cloud computing-based vehicle control, and active suspension control.